Order and Chaos in the One-Dimensional ϕ^4 Model :
N-Dependence and the Second Law of Thermodynamics

William Graham Hoover

Ruby Valley Research Institute

Highway Contract 60, Box 601

Ruby Valley, Nevada 89833

and Kenichiro Aoki

Department of Physics, Hiyoshi Campus, Keio University

Hiyoshi, Yokohama 223, Kanagawa, Japan

(Dated: February 7, 2017)

Abstract

We revisit the equilibrium one-dimensional ϕ^4 model from the dynamical systems point of view. We find an infinite number of periodic orbits which are computationally stable. At the same time some of the orbits are found to exhibit positive Lyapunov exponents! The periodic orbits confine every particle in a periodic chain to trace out either the same or a mirror-image trajectory in its two-dimensional phase space. These "computationally stable" sets of pairs of single-particle orbits are either symmetric or antisymmetric to the very last computational bit. In such a periodic chain the odd-numbered and even-numbered particles' coordinates and momenta are either identical or differ only in sign. "Positive Lyapunov exponents" can and do result if an infinitesimal perturbation breaking a perfect two-dimensional antisymmetry is introduced so that the motion expands into a four-dimensional phase space. In that extended space a positive exponent results.

We formulate a standard initial condition for the investigation of the microcanonical chaotic number dependence of the model. We speculate on the uniqueness of the model's chaotic sea and on the connection of such collections of deterministic and time-reversible states to the Second Law of Thermodynamics.

Keywords: Molecular Dynamics, Lyapunov Instability, Time-Reversible Thermostats, Chaotic Dynamics

1

I.   INTRODUCTION

The study of an anharmonic heat-conducting lattice-dynamics model, the ϕ^4 model, from the standpoint of classical statistical mechanics was explored by Aoki and Kusnezov[1,2] and by Hu, Li, and Zhao[3] in 2000. The Aoki-Kusnezov work led to particularly clear and easily reproducible illustrations of the phase-space dimensionality loss found in nonequilibrium steady states as was discussed and illustrated with Holian, Hoover, Moran, and Posch in 1987[4-6]. Unlike the harmonic chain, in which heat travels ballistically at the speed of sound, the one-dimensional ϕ^4 model exhibits Fourier heat conductivity with a finite large-system limit. This difference to the harmonic chain is due to the presence of quartic "on-site" "tethering" potentials, one for each particle. These tethers suppress the amplitude of low-frequency waves. We will see that there is a relatively wide number-dependent energy range within which the tethers induce a chaotic dynamics.

The Hamiltonian for the one-dimensional ϕ^4 model is the sum of the kinetic, tethers, and nearest-neighbor pair-potential energies :

$$\mathcal{H} = K + \Phi_{\text{tethers}} + \Phi_{\text{pairs}} = \sum_i^N [\ (p_i^2/2) + (q_i^4/4)\ ] + \sum_{i<j}^{\text{pairs}} (q_i - q_j)^2/2 \ .$$

Here the $\{\ q\ \}$ represent the displacements of the particles from their static lattice rest positions. The $\{\ p = \dot{q}\ \}$ are the corresponding momenta. The rest length d of the Hooke's-Law springs is irrelevant in this one-dimensional case where it makes no contribution to the pair-potential part of the equations of motion :

$$\ddot{q}_i + q_i^3 = (i+1)d + q_{i+1} - 2(id + q_i) + (i-1)d + q_{i-1} \equiv q_{i+1} - 2q_i + q_{i-1} \ .$$

Free, fixed, and periodic boundary conditions are all possibilities. We mostly choose the periodic case in which the first and last particles in the chain are linked by a Hooke's-Law spring so that the resulting "loop" is homogeneous and periodic.

Ever since their 1987[4,5] work with Brad Holian and Bill Moran, Harald Posch and Bill Hoover sought clearcut evidence that the fractal nature of nonequilibrium phase-space distributions found for small systems persists in larger ones. The fractal phase-space structures can be used to explain the Second Law of Thermodynamics in purely mechanical terms for both microscopic and macroscopic systems. The fractals not only show the measure-zero nature of nonequilibrium steady states. They also clarify the irreversible nature of the uni-directional repellor-to-attractor phase-space flow. This Second Law connection to fractal

structures can best be established through studies of the dynamical instabilities described by the Lyapunov spectrum[6–11].

The Lyapunov spectrum $\{ \lambda_i \}$ has a number of exponents equal to the dimensionality of the phase space, for which we use the symbol D . The exponents describe the virtual growth and decay rates parallel to the orthogonal axes of a comoving and corotating phase-space hypersphere. The exponents are ordered according to their long-time-averaged values, beginning with the largest, λ_1 and ending up with the smallest λ_D . λ_1 describes the time-averaged rate at which two nearby trajectories tend to separate , $\lambda_1 = \langle \dot{\delta}/\delta \rangle$. We call these rates "virtual" because the numerical algorithms used to measure them maintain trajectory separations by rescaling or by using Lagrange-multiplier constraints[8]. Sums of the first n exponents describe the growth and decay rates of n-dimensional comoving and corotating phase-space balls. In the equilibrium case of pure Hamiltonian mechanics Liouville's Theorem, $\dot{f}(t) \equiv 0$, along with the comoving conservation of the phase-space probability, $f\otimes$, implies that the sum of all the Lyapunov exponents is precisely zero :

$$\dot{f} = 0 \text{ and } (d/dt)(f\otimes) \equiv 0 \longrightarrow \dot{f} \otimes + f\dot{\otimes} = 0 + 0 \longrightarrow \dot{\otimes} = 0 .$$

$$\langle (\dot{f}/f)_t \rangle = \langle [(\dot{f}(t)/f(t)] \rangle = -\langle (\dot{\otimes}(t)/\otimes)(t) \rangle = \langle -\sum_i^D \lambda_i(t) \rangle = -\sum_i^D \lambda_i \equiv 0 .$$

Here $\lambda_i(t)$ is the ith instantaneous exponent and λ_i is its time average. Hamiltonian long-time-averaged exponents occur in equal and opposite pairs, $\{ \pm\lambda \}$, corresponding to the time reversibility of the motion equations. Expansion and contraction exchange places in a reversed Hamiltonian flow. **Figure 1** shows the 32 Lyapunov exponents for two periodic 16-particle ϕ^4 chains. In both cases the two vanishing exponents correspond to the lack of growth or decay in the direction of the phase-space trajectory and in the direction perpendicular to the 32-dimensional energy surface $E = \mathcal{H}$.

The nonequilibrium case is quite different[4–6,9–11]. It does seems likely that this ϕ^4 model will prove useful for future nonequilibrium studies involving the thermodynamics of heat transfer. Accordingly we review our current knowledge of nonequilibrium aspects of the model here. Velocity gradients or thermal gradients induced or maintained by deterministic thermostats invariably lead to a breaking of time symmetry. Away from equilibrium the thermostated time-averaged rate of change of the phase volume $\langle \dot{\otimes} \rangle$ is invariably negative. The thermostated phase volume shrinks onto a stationary strange attractor. The attractor
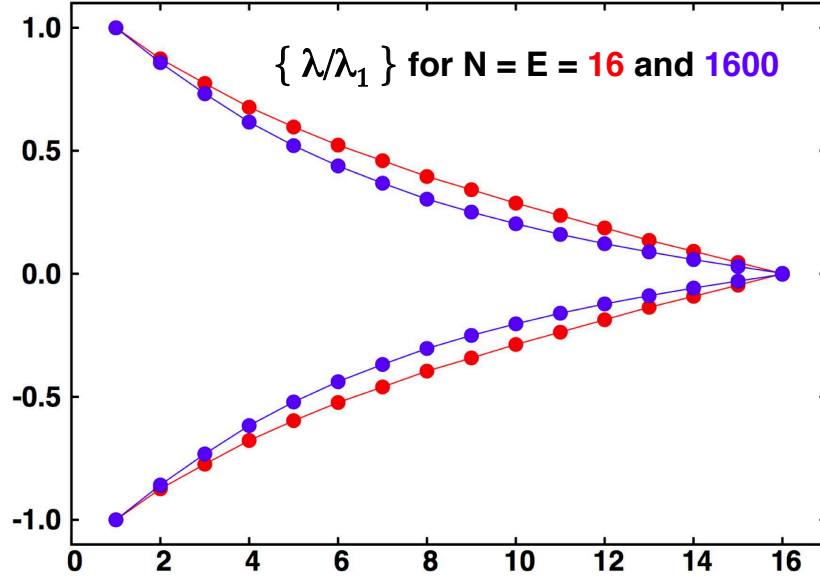
FIG. 1: The 16 pairs of Lyapunov exponents for chaotic and periodic 16-body ϕ^4 chains, "loops", with $(E/N) = 1$ and 100 . The spectra have been divided by the largest Lyapunov exponents, $\lambda_1 = 0.0746$ and 0.242 , respectively. The red/blue points correspond to 16/1600 respectively.

has a *fractional* "information dimension" D_I less than that of the phase volume, D . The information dimension involves a sum over phase-space bins of linear size ϵ :

$$D_I = \sum_{\text{bins}} [\, P \ln(P) / \ln(\epsilon) \,] \; (\text{ in the small}-\epsilon \text{ limit }) .$$

The bin probabilities are normalized : $\sum P \equiv 1$.

A direct measurement of the information dimension is impractical for problems with more than three or four phase-space dimensions because the number of bins becomes prohibitive. Accordingly Kaplan and Yorke suggested a handy approximation D_{KY} to the information dimension : The Kaplan-Yorke approximation is determined by linear interpolation between the dimensionality of the highest-dimensional expanding ball (D_e) and the dimensionality

of the lowest-dimensional contracting ball $D_c = (D_e + 1)$:

$$\sum_i^{D_e} \lambda_i > 0 > \sum_i^{D_e+1} \lambda_i = \sum_i^{D_c} \lambda_i \longleftrightarrow D_e < D_{KY} \simeq D_I < D_c = D_e + 1 \ .$$

When $\lambda_1 > 0$ and the "Kaplan-Yorke" fractal dimension D_{KY} of the distribution is less than that of the phase space the distribution of trajectory points occupies a "strange attractor". In such cases, the probability of finding states violating the Second Law of Thermodynamics *vanishes* rather than just being small[4]. The "volumes" of fractals are *zero* in their embedding spaces.

Aoki and Kusnezov's ϕ^4 model provides many far-from-equilibrium examples of the relatively large dimensionality loss $\Delta D = D - D_I \simeq D - D_{KY}$. For example two-dimensional square-lattice ϕ^4 models with 64, 100, and 144 particles, with one corner hot and another, diagonally opposite, cold, gave dimensionality losses ΔD of 12.5[6], 21.6[10], and 33.8[10]. In their recent book the Hoovers extended the one-dimensional calculations to 24- and 32-particle chains with dimensionality losses of $\Delta D \simeq 35$ out of 48+2 and $\Delta D \simeq 43$ out of 64+2 phase-space dimensions[11].

In the present work we characterize the Lyapunov instability of equilibrium loops and chains from the standpoint of dynamical systems theory, seeking to outline the region in which chaos is present and to explore its characteristics. In Section II we consider a standard initial state and discuss tests for chaos based on the largest Lyapunov exponent and the distribution of kinetic temperature $\{ p^2 \}$. Detailed results are given in Section III. Our conclusions and recommendations for further work are summarized in Section IV.

II. A CONVENIENT INITIAL CONDITION FOR CHAOTIC CHAINS

The restlength of the nearest-neighbor springs is irrelevant in one dimension. Without loss of generality it can be chosen equal to zero with the $\{ q \}$ representing displacements about a common origin. Evidently ϕ^4 thermodynamics depends upon only one intensive variable, the internal energy (E/N) [or, equally well, the kinetic temperature, $\langle p^2 \rangle$, or the specific potential energy, (Φ/N)] but *not* at all upon a specific volume (length) or density variable. To choose an initial condition consistent with a particular conserved energy E it is simplest to follow a two-step process. First, choose all of the N momenta randomly, using the random number generator described below. The sign of the momenta is unimportant as

momentum is not conserved by the ϕ^4 model. Next, rescale the momenta so as to generate the desired initial energy E . Initially, but not for long, the total energy is all kinetic : $E = K_{t=0} = \sum(p^2/2)_{t=0}$. For convenience in our numerical work we choose the mass and Boltzmann's constant both equal to unity and integrate the equations of motion with a fourth-order Runge-Kutta integrator, choosing the timestep such that the rms single-step integration error is of order 10^{-10} . In doubtful or surprising cases an adaptive integrator comparing the integration over a timestep dt to two successive integrations with timesteps $(dt/2)$ is useful.

An alternative to Hamiltonian mechanics is "thermostated" mechanics which by now has a huge 30-years' literature. We choose to use the simplest possible (Nosé-Hoover) thermostat(s). To thermostat an N-body periodic ϕ^4 loop it is only necessary to thermostat one of the N particles at the desired temperature T. In nonequilibrium simulations it is usual to thermostat two particles, one "hot" and one "cold", at the two ends of an N-body chain. The equations of motion for any thermostated particle, either at equilibrium or away, include an extra thermostat force imposed by a friction coefficient or "control variable" ζ :

$$F_{\mathrm{NH}} = -(\zeta p)_{\mathrm{NH}} \; ; \; \dot{\zeta}_{\mathrm{NH}} = p_{\mathrm{NH}}^2 - T_{\mathrm{NH}} \; [\; \mathrm{Nos\acute{e}} - \mathrm{Hoover \; Thermostat} \;] \; .$$

We will apply this thermostat to our equilibrium simulations in Section IIID.

A.   Definition of Kinetic Temperature Through the Ideal-Gas Thermometer

The definition of "kinetic temperature" $\langle \; p^2 \; \rangle \equiv T$ and our exclusive use of that temperature in this work, is based on the thermodynamic definition of temperature in terms of an ideal-gas thermometer. Conceptually such a thermometer is made up of many tiny fast-moving particles. Frequent collisions ensure that the thermometer has always a Maxwell-Boltzmann distribution of momenta, $f(p) \propto e^{-p^2/2T}$. It is a straightforward kinetic-theory exercise to show that a massive particle's interaction with such a thermometer results in a frictional force on the heavy particle, proportional to its velocity. Further a similar calculation for our one-dimensional case shows that a heavy particle loses energy to an ideal-gas thermometer if its mean squared velocity exceeds (kT/M) where T is the ideal-gas temperature and M is the massive particle's mass[13]. Likewise the heavy particle gains energy if (kT/M) exceeds its mean squared velocity. Defining the temperature of a particle as

that of the thermometer which neither gains nor loses energy due to collisions provides an unambiguous mechanical definition of that particle's temperature. This definition is fully consistent with equilibrium thermodynamics and also facilitates the analysis of nonequilibrium situations involving one or more heat reservoirs. Such reservoirs are simply large versions of the ideal-gas thermometer.

B. Definition and Computation of the Largest Lyapunov Exponent

In any case, at a fixed energy E, or thermostated at one equilibrium temperature T, or at two nonequilibrium temperatures $T_{\text{hot and cold}}$, there are at least four distinct ways to determine the largest Lyapunov exponent. From the conceptual standpoint all four involve following the motion of two similar systems, the "reference" trajectory which is unperturbed, and a nearby "satellite", which is constrained to evolve at a fixed separation from the reference. The satellite trajectory can be described in phase space (by solving identical equations of motion) or in "tangent space" where the offset is infinitesimal and the satellite equations of motion are linearized with respect to the offset, $\{ \delta q, \delta p, \delta \zeta \}$. The constant-offset constraint can be imposed by rescaling at the end of every timestep or by including an extra Lagrange multiplier[7,8] in the satellite motion equations. For finite separation a convenient choice is

$$\delta = 0.000001 = \sqrt{\sum [(q_s - q_r)^2 + (p_s - p_r)^2] + (\zeta_s - \zeta_r)^2 } \; .$$

We have used both phase-space and tangent-space methods, both fixed timestep and variable-timestep Runge-Kutta integrators, compiled from both FORTRAN and C in order to check our work. For more details of the Lyapunov algorithms and several examples see Chapter 5 of Reference 11 or the many papers on this subject in the Los Alamos arχiv.

C. Random Number Generator

In many of our simulations we have used the six-line random number generator `rund(intx,inty)` with the two seeds `intx` and `inty` initially set equal to zero. This generator is time-reversible[12]. Its forward version is as follows :

```
i = 1029*intx + 1731
j = i + 1029*inty + 507*intx - 1731
intx = mod(i,2048)
j = j + (i - intx)/2048
inty = mod(j,2048)
rund = (intx + 2048*inty)/4194304.0
```

$2^{22} = 4194304$ pseudorandom numbers are generated before the algorithm repeats.

We recommend the use of this six-line generator for three reasons : [1] it is simple to implement ; [2] it is reproducible, so that colleagues working with different hardware or software can readily replicate each others' work ; [3] it is "time-reversible" so that the seed-dependent sequence of 2^{22} pseudorandom numbers can be extended either forward or backward in "time". This last property of time reversibility was established by Federico Ricci-Tersenghi in his solution of the 2013 Ian Snook Prize Problem[12]. This property makes it possible to follow "stochastic" evolutions of few-body or many-body dynamics backward in time .

At sufficiently low temperatures where the quartic potential can play no role the ϕ^4 model motion becomes harmonic. In this case the lowest frequency corresponds to a wavelength of N for periodic boundary conditions and $2N + 2$ for fixed boundaries, with just N motion equations for the coordinates and for the momenta. We have also used free boundaries at the endpoints which likewise have N equations each for the coordinates and momenta. The amplitude of the harmonic motion follows from the harmonic oscillator relation for a vibrational normal mode of frequency ω with the energy equally divided among the system's N modes :

$$\sqrt{\langle\, q^2\, \rangle = (kT/m\omega^2)} \simeq \sqrt{(E/N)(2N)^2} \simeq \sqrt{(EN)} \simeq \sqrt{TN^2}\ .$$

At temperatures T higher than $(1/N^2)$ the long wavelength harmonic waves are scattered to higher frequencies by the tethering potentials.

D. Monte-Carlo Determination of the Chaotic Measure

Over most of the energy range chains or loops of length 8 or more are typically chaotic, but this cannot be the case at very low or very high energies. To determine the relative

measures of the tori and the chaotic sea we have used the following idea :

[1] Use scaled random numbers from the generator in the previous section to start a simulation with a desired energy, initially wholly kinetic.

[2] Measure the Lyapunov exponent for 2 000 000 000 timesteps.

[3] Make $(N/2)$ vectors of length $r = | (p_i - p_{i+1}) |$ with the $(N/2)$ distinct pairs (where i is odd) of adjacent momenta, rotate each vector through a random angle θ between 0 and $(\pi/2)$. Setting the momenta equal to $[r\sin(\theta), r\cos(\theta)]$ provides a new initial condition with the same energy as before.

[4] Repeat steps 2 and 3 above for a sufficient number of trials (40 is reasonable).

Because this procedure satisfies ergodicity (any isoenergetic configuration is able to be accessed) and "detailed balance" (the probability of going from state I to state J is the same as that from J to I) because the algorithm is time reversible. Thus its implementation will ("eventually") converge to Gibbs' microcanonical (constant-energy) average. Let us turn to an exploration of results obtained with the methods just described. Our main goal is to determine the extent of the chaos in the ϕ^4 model. In the course of that work we encountered several surprises. They are included in what follows.

III.   NUMERICAL RESULTS

Figure 2 shows the dependence of the largest Lyapunov exponent on (E/N) for $N = 16$ and $N = 500$. These systems are sufficiently large and energetic that our standard initial condition leads to chaos over a wide range of energies. It is remarkable that the simple ϕ^4 model has a readily-accessible chaotic range of about ten orders of magnitude in the energy.

A.   The Equilibrium Thermal Equation of State

At very low temperatures the motion is harmonic so that the energy approaches the equipartition result, $(E/2) = K = \Phi = NT/2$, where K and Φ are the kinetic and potential energies. In the opposite high-temperature limit,

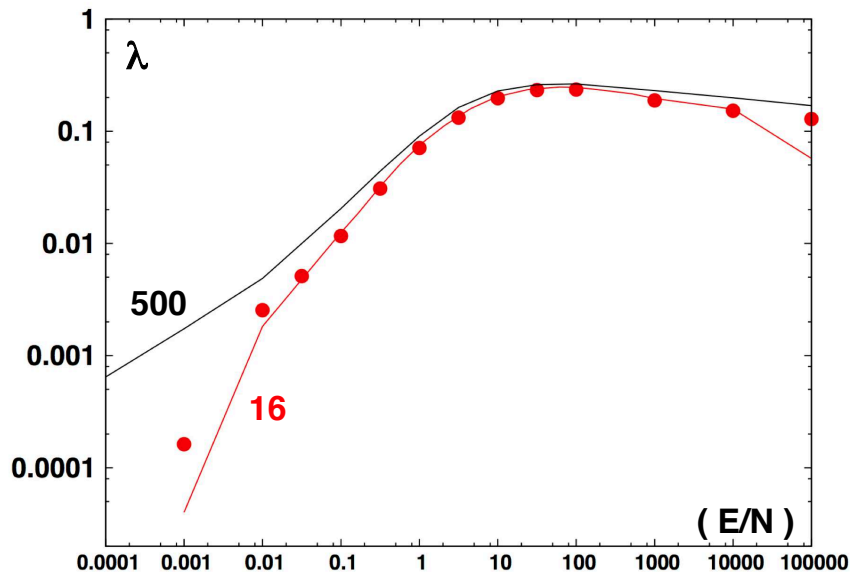$$\langle (q^4/4) \rangle \simeq T \rightarrow \Phi \simeq (NT/4) .$$

FIG. 2: The energy dependence of the largest Lyapunov exponent for periodic systems of 16 and 500 particles are shown as lines. Data using fixed boundary conditions with 16 moving particles and two fixed boundary particles are shown as filled circles. All these simulations were initiated with vanishing coordinates $\{ q \}$ and with randomly chosen initial velocities scaled to provide the desired energy. The trajectories were integrated for sufficient time that the uncertainties in the $\{ \lambda_1 \}$ are smaller than the size of the filled circles.

For orientation notice that **Figure 3** shows that the kinetic and potential energies satisfy equipartition (they are equal) at low temperature. At high temperature where the configurational integral $\int e^{-\Phi/kT} dq \simeq T^{1/4}$ the slope, $d\Phi/dT$ changes from $(1/2)$ to $(1/4)$. For the plot we have used states from the chaotic sea. From the *rigor mortis* standpoint there are also an infinite number of zero-measure periodic orbits, mostly unstable. Some of them are stable, surrounded by small-measure families of tori. We will encounter both the unstable and the stable cases in studying the smallest interesting case, $N = 2$.
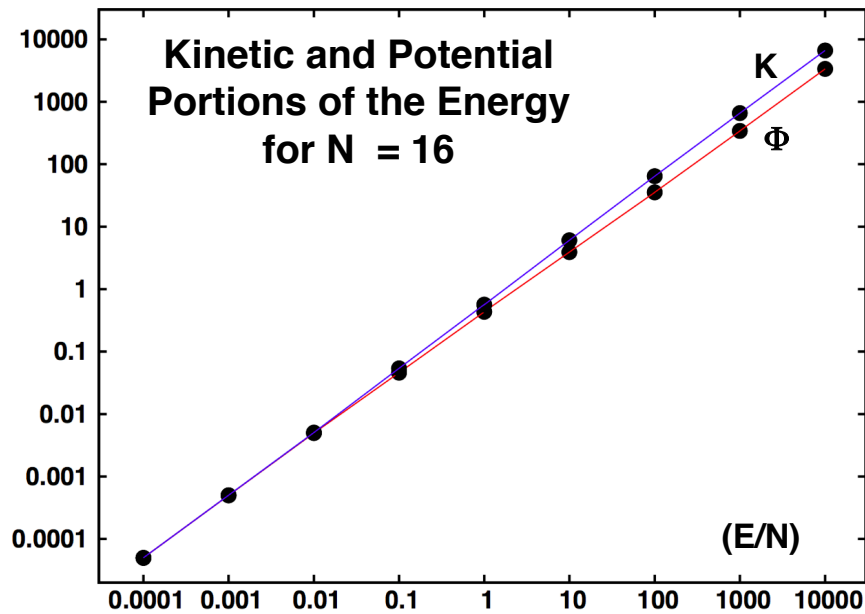
10

FIG. 3: The upper curve shows the variation of kinetic energy per particle and the lower curve the variation of potential energy per particle with the abscissa values of the total energy per particle. The low-temperature equipartition and the high-temperature ratio of energies correspond to harmonic motion and quartic-potential oscillation respectively. The data were taken from periodic simulations with $N = 16$.

B. $N = 2$, the Minimal Case for Chaos

We begin with the smallest system for which chaos is possible, a pair of one-dimensional particles. We choose to examine the periodic case, imagining that there are two parallel Hooke's-Law springs joining the pair :

$$\mathcal{H} = (1/2)(p_1^2 + p_2^2) + (q_1 - q_2)^2 + (1/4)(q_1^4 + q_2^4) .$$

11

With the energy fixed by the Hamiltonian motion equations this four-dimensional problem has the minimum dimensionality for chaos, three. "Obviously" solutions with either of the two symmetry choices $(q_1, p_1) = \pm(q_2, p_2)$ are "too simple for chaos". To see this consider first the symmetric case and set $(q, p) = (q_1, p_1) = (q_2, p_2)$. The motion equations are the same for the two particles :

$$\dot{q} = p \; ; \; \dot{p} = -q^3 \; .$$

This same result holds for a periodic chain made up of any even number of particles. In this "symmetric" case, with all the particles tracing out the same (q, p) motion the nearest-neighbor Hooke's-Law potential is constant with its minimum value of zero. Only the onsite quartic potential is nonzero. These are the motion equations in a simple attractive quartic potential.

The "antisymmetric" case, corresponding to mirror boundary conditions, looks similar. For two particles or any other even number, all particles obey the same motion equations :

$$\dot{q} = p \; ; \; \dot{p} = -4q - q^3 \; .$$

This antisymmetric case describes periodic oscillations in an attractive potential only slightly more complicated than the symmetric case. (q, p) phase-plane plots of both periodic orbits are shown in **Figure 4**. To avoid overlaps the particle coordinates q_1 and q_2 have been shifted to the left and right by 3 .

From the mathematical standpoint the symmetric and the antisymmetric problems are both equivalent to one-body problems tracing out periodic orbits in a two-dimensional (q, p) phase space and as such are immune to chaos. But this brief discussion ruling out chaos in two dimensions is completely erroneous in four! After all it seems possible that the symmetric and antisymmetric orbits in the original four-dimensional phase space could themselves be unstable to small perturbations which are inaccessible in the simpler two-dimensional symmetrized spaces. In such a case double-precision roundoff errors *might* be enough to provide a seed for instability on the three-dimensional (as opposed to one-dimensional) energy surface. Numerical exploration shows that an energy $E = 15$ is enough for chaos with a positive λ_1 in the full four-dimensional (q_1, p_1, q_2, p_2) space.

If we start out with the antisymmetric initial condition of **Figure 4** we find rapid con-
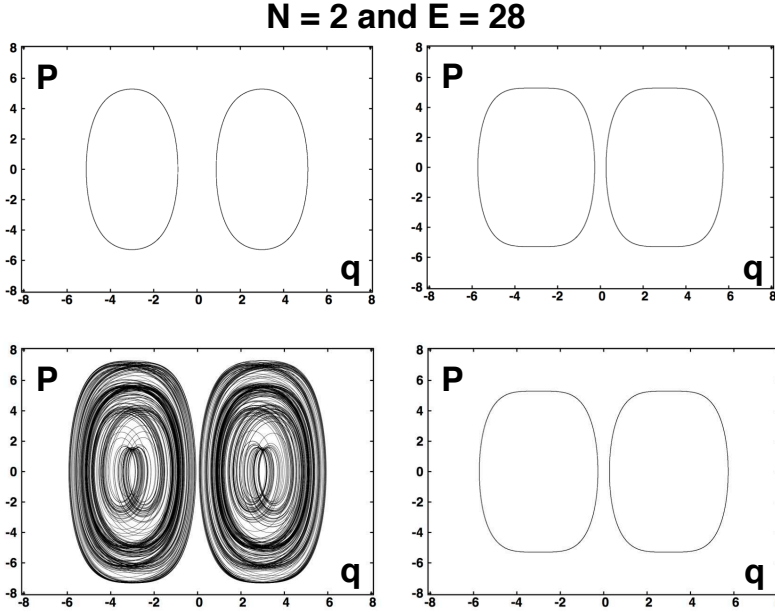
N = 2 and E = 28

FIG. 4: The antisymmetric (on the left) and symmetric (on the right) phase-plane orbits are In the symmetric case, with all particles tracing out the same (q,p) motion the nearest-neighbor Hooke's-Law potential is constant with its minimum value of zero. Only the onsite quartic potential is nonzero, as is shown here for an energy of 28. Both of the top-row orbits, as well as their periodic repetitions, are computationally stable to the very last bit. In contrast, adding a small perturbation to any of the four variables opens up a four-dimensional phase space and reveals that the antisymmetric case is then Lyapunov unstable (as shown below at the left). The symmetric case remains stable, revealing the existence of a torus with nonzero measure in that symmetric case.

vergence of the largest Lyapunov exponent to a value of order unity :

$$\{ \ q_1, p_1, q_2, p_2 \ \} \simeq \{ \ +2, +2, -2, -2 \ \} \longrightarrow \lambda_1 = 0.617 \ .$$

Apart from a phase shift we expect this initial condition to correspond equally well to the purely-kinetic initial condition. Computation shows that this is true :

$$\{ \ q_1, p_1, q_2, p_2 \ \} \simeq \{ \ 0, +\sqrt{28}, 0, -\sqrt{28} \ \} \longrightarrow \lambda_1 = 0.617 \ .$$
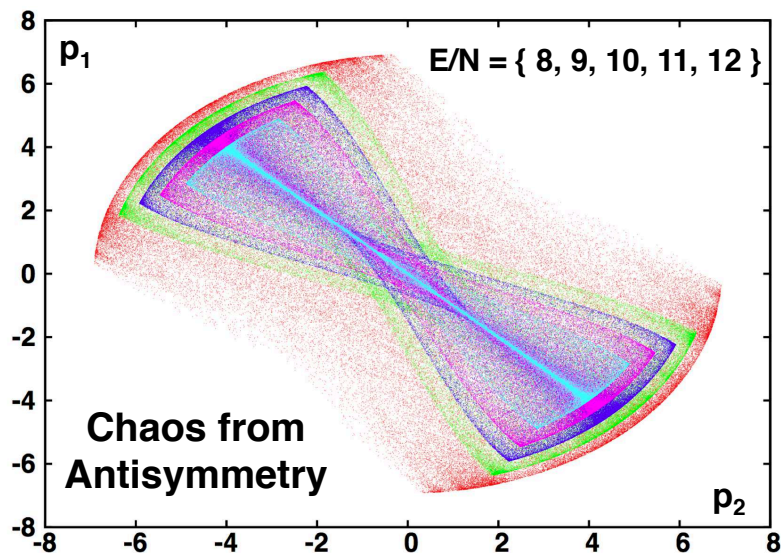
FIG. 5: Antisymmetric chaos broadens the correlation of the momenta $p_1 + p_2 = 0$ as the energy is increased. The two momenta are plotted for energies of 16, 18, 20, 22, and 24. The transition from order to chaos occurs near $E = 15$.

The Runge-Kutta integrator, as interpreted by FORTRAN or C is certainly not perfect in a mathematical sense. It isn't even time-reversible. But it does preserve *symmetry* very nicely (even perfectly) as a consequence of arithmetic operations where only the sign of the numbers is changed. This symmetry can be lost if the rest lengths of the springs are incorporated in the equations of motion. *Displacement* coordinates { q } are advantageous !

Figure 5 illustrates the growth of chaos in the unstable antisymmetric case. At low energy the momenta p_1 and p_2 sum to zero in a regular periodic motion. Increasing energy eventually breaks the perfect correlation and gives rise to the increasing chaos seen in the Figure. For energies less than fifteen, so that $(E/N) < 7.5$, the $p_2(p_1)$ correlation is perfect, corresponding to the straight line $p_1 + p_2 = 0$.
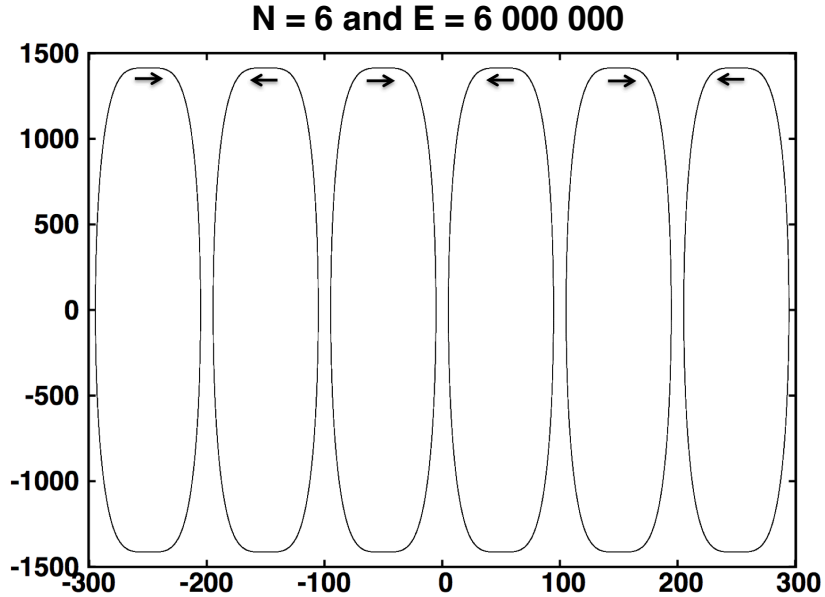
FIG. 6: The antisymmetric (q, p) solution applies to any even number of ϕ^4 particles. Here we show the (offset to avoid overlaps) phase-plane plots for a periodic system of six particles. We emphasize the perfect computational stability, to the very last bit, of such an orbit. The case illustrated has $(E/N) = 1,000,000$. The corresponding maximum Lyapunov exponent is 1.153 .

C. Anomalous Orbits for More Pairs of Particles

It is easy to verify that simulations repeating the same starting condition as above,

$$\{ q, p, q, p \} = \{ +2, +2, -2, -2, +2, +2, -2, -2, +2, +2, -2, -2, \ \ldots \ \} \ ,$$

where $N = 2, \ 4, \ 6, \ \ldots$ all give exactly the same (q, p) plots for every particle and all give exactly the same Lyapunov exponent, $\lambda_1 = 0.617$ for $(E/N) = 14$. See **Figure 6** for $(E/N) = 1,000,000$.

What is a bit surprising is that a small perturbation, say 10^{-15} , totally changes things. A

15

nonzero perturbation out of the (q, p) plane can break the antisymmetry. Such a perturbation provides a Lyapunov exponent that is not particularly stable and is considerably smaller, on the order of 0.1 , than the exponent on the unperturbed periodic orbit. Evidently the precisely antisymmetric simulations, without perturbations, differ only in the signs of the (q, p) not the magnitudes. Thus standard double-precision arithmetic can maintain perfect antisymmetry and periodicity with no hint of chaos. On the other hand the nearby (perturbed) satellite trajectory senses a Lyapunov exponent of 0.617 . That exponent has nothing to do with a chaotic-sea average. It is instead simply the mean value of $\lambda_1(t)$ adjacent to the underlying periodic orbit. The symmetric case is less interesting. Even with an energy of 10^6 the symmetric Lyapunov exponent is only 0.03. With an energy of 10^5 the exponent is negligibly small, most likely zero.

For comparison we include another initial condition, neither symmetric nor antisymmetric, but still with the same initial energy $(E/N) = 14$:

$$\{ q_1, p_1, q_2, p_2 \} \simeq \{ +2, +2, -2, +2 \} \longrightarrow \lambda_1 = 0.08_6 \ ,$$

This initial condition evidently samples the chaotic sea rather than just the neighborhood of a periodic orbit (we avoid calling the periodic orbits "stable" or "unstable" as this is not useful terminology in the two-body case). An antisymmetric initial condition with a smaller perturbation should (we think) sample the same chaotic sea. The result of a computation with a billion timesteps of 0.001 each is $\lambda_1 = 0.08_8$, justifying our expectation. In summary the two-particle case (and the $2N$-particle cases) exhibit something interesting, a periodic orbit periodic to machine precision, stable computationally for so long as the electricity flows, but in the neighborhood of a highly-unstable portion of the chaotic sea.

A little reflection suggests that there may well be families of periodic orbits related to all the normal modes of a chain. The next step up from $N = 2$ is $N = 3$, which exhibits a computationally perfect symmetry of the type

$$(0, \ +2, \ -2) = (p_1, \ p_2, \ p_3) \text{ with } (q_1, \ q_2, \ q_3) = (0, \ 0, \ 0) \longrightarrow \mathcal{H} = 4 \ .$$

This robust periodic solution has a Lyapunov exponent of 0.13_6, the same order of magnitude as in the similar two-body solution. Because the first particle is motionless such a solution satisfies both the periodic and the fixed boundary conditions. Such stable periodic orbits with positive Lyapunov exponents are a fertile field for additional research. Without

pursuing that subject further here we turn now to another more manageable set of interesting problems, loops with $N = 10,\ 20,\ 40,\ 80,\ 160$ and their approach to the large-system limit.

D. Number-Dependence for Longer Chains and Loops

With longer chains a systematic number dependence of λ_1 can be seen. Seeking simplicity we begin with periodic chains for which the boundary conditions are homogeneous and do not single out any part of the system. For unit energy per particle, $(E/N) = 1$ and in the chaotic sea, we computed the kinetic energy per particle and the maximum Lyapunov exponent for ϕ^4 loops of 10, 20, 40, 80, and 160 particles. All of these systems exhibit a kinetic temperature close to an apparent longchain limit of 1.134 . Simulations were carried out using two billion timesteps with a fourth-order Runge-Kutta timestep $dt = 0.001$. The per-particle kinetic energies and Lyapunov exponents we found were as follows :

$$(K/N) = \{\ 0.566_2,\ 0.566_3,\ 0.567_0,\ 0.567_0,\ 0.567_0\ \}\ ;$$

$$\lambda_1 = \{\ 0.0666,\ 0.0767,\ 0.0810,\ 0.0843,\ 0.0871\ \}\ .$$

The Lyapunov exponents vary roughly linearly in the inverse loop size while the kinetic energy (or temperature) has a variation smaller by two orders of magnitude. The 31% increase in λ_1 is huge relative to the tiny increase in temperature with a sixteenfold increase in system size.

To test the sensitivity of the Lyapunov exponent to thermostating we added a single Nosé-Hoover control variable to the motion equations of a single particle and verified that the chains all came to thermal equilibrium at a kinetic energy of unity with the motion equation of Particle 1 modified as follows :

$$\dot{p}_1 = \dot{p}_1(\mathcal{H}) - \zeta p_1\ ;\ \dot{\zeta} = p_1^2 - 1\ .$$

The Lyapunov exponents for the thermostated chain at a kinetic temperature of 1 found in this way were :

$$\lambda_1 = \{\ 0.0791,\ 0.0826,\ 0.0833,\ 0.0841_6,\ 0.0844_5\ \}$$
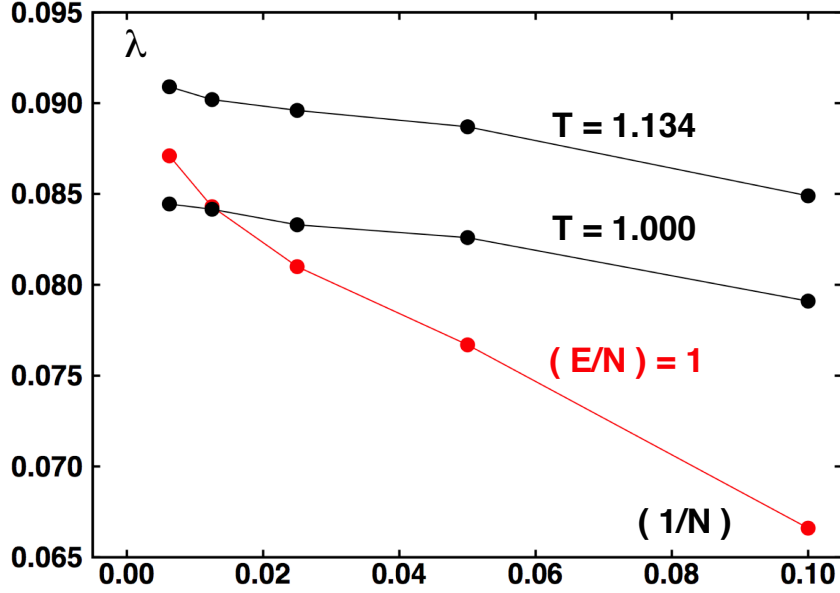
FIG. 7: These data indicate that the number dependence of the largest Lyapunov exponent is of order $(1/N)$. The steepest curve is for Hamiltonian mechanics with an energy per particle of unity. The other curves shows $\lambda_1(N)$ for the same system sizes, 10, 20, 40, 80, and 160 particles with a single particle thermostated at a temperature of 1.134 (at the top) and at a temperature of unity (below). The equations of motion for the lone thermostated particle include the frictional force $-\zeta p$ where $\dot{\zeta} = p^2 - 1.134$ or $p^2 = 1.000$. All these data represent time averages in the chaotic sea with two billion timesteps, $dt = 0.001$.

At the temperature 1.134 corresponding to unit energy per particle the largest Lyapunov exponent is somewhat larger, as is shown in **Figure 7** :

$$\lambda_1 = \{\ 0.0849,\ 0.0887,\ 0.0896,\ 0.0902,\ 0.0909\ \}$$

In the present calculations we used $\dot{\zeta} = p^2 - T$ rather than the alternative $\dot{\zeta} = (p^2/T) - 1$.

E. Dependence of the Chaos on Energy

Figure 2 illustrated the dependence of the largest Lyapunov exponent on the specific energy (E/N). The falloff at low energy, and eventual disappearance of the chaotic sea corresponds to the normal-mode structure of the low-energy ϕ^4 model. At very low energy, $E \simeq NT < (1/N)$, the initial conditions correspond to the amplitudes and phases of N normal modes, all of which are periodic in time so that there is no tendency toward chaos. At very high energy, where the Hooke's-Law forces can be ignored relative to the tether forces each particle oscillates about its lattice site with a regular periodic one-dimensional motion. For these reasons the "interesting" chaotic range of energies considered here cover nine orders of magnitude.

The relative measures of the chaotic sea and regular tori vary with system size and with energy, from (0,1) to (1,0) to (0,1) as the energy varies from zero to order one to infinity. We have used the Monte Carlo method of Section II.D to determine the chaotic energy for a sixteen-particle loop, which **Figure 2** showed us is already close to the large-system limit. At an energy (E/N) = 1,000,000 the Monte Carlo algorithm returns a chaotic measure of 14/40 . In the range 0.1 to 1000 all 40 initial conditions in our microcanonical sample were chaotic. Apart from an early transient (indicating some regular measure) in the Monte Carlo samples with $(E/N) = 0.01$ and 0.001 the measure there is overwhelmingly chaotic too.

F. Uniqueness and Equilibration of the Chaotic Sea

The realism of the ϕ^4 model is amazing considering its simplicity. By considering hundreds of different initial conditions, randomly chosen but otherwise with equal energies we have reached the conclusion that the chaotic sea is likely unique. Given the number of particles and the energy it appears that there is only one chaotic sea, not two or three or an infinite number. Further by considering a more limited number of chaotic states it appears that their kinetic temperature converges homogeneously :

$$\langle\, p_1^2 \,\rangle = \langle\, p_2^2 \,\rangle = \ldots = \langle\, p_N^2 \,\rangle \ .$$

Without robust thermal equilibrium in the sea we would have to consider the embarassing possiblity of a violation of the Second Law of Thermodynamics, as is discussed below among

the conclusions and recommentations which have come to us through our studies and to which we turn next.

IV.   CONCLUSIONS AND RECOMMENDATIONS

The ϕ^4 model provides a readily reproducible set of chaotic few-body and many-body problems where interference from toroidal solutions is minimal. There is room for work leading to a quantitative understanding of the first appearance of chaos at low energies and its last vestige at high. Preliminary explorations indicate that the number of nonvanishing exponent pairs varies with energy in the vicinity of the antisymmetric unstable orbit.

The symmetric and antisymmetric two-body solutions, with the surprising coexistence of computational stability adjacent to Lyapunov instability was unexpected. Although the chaotic sea is a close neighbor to these solutions the identical roundoff errors for all the even and all the odd numbered particles provides stability adjacent to chaos. No doubt other more complex patterns are stabilized by the same roundoff mechanism, providing nonlinear analogs of the harmonic normal modes. By adding dissipative friction to the motion equations the fundamental long wavelength modes could be captured for any of the choices of boundary conditions, periodic, fixed, or free.

The mechanical model exhibiting heat flow in response to kinetic temperature gradients facilitates studies connecting mechanics to thermodynamics. Because thermodynamics is based on the ideal gas, with its known Gaussian velocity distribution, entropy, and temperature links to mechanical systems capable of heat transfer for very small N^{14} are appealing subjects for computational study.

It seems likely to us (we have so far found no counterexample) that simulations in the chaotic sea correspond to global microcanonical thermal equilibria despite their finite energy and the closeby regular tori with their nonchaotic quasiperiodic time behavior. Gibbs' maximum-entropy velocity distribution can be separated from the highly complex configurational component of the energy surface. We conjecture that over a wide range of energies there is a unique chaotic sea in which all particles share a common value of the kinetic temperature $\langle p^2 \rangle$. If chaotic solutions were able to provide reproducibly different kinetic temperatures $\langle p^2 \rangle$ in different parts of a microcanonical system it would be possible to violate the Second Law of Thermodynamics by coupling an external Carnot Cycle to those

energy sources and sinks, for the Carnot cycle feeds on the kinetic energy by exactly the same collisional mechanism as the measurement mechanism of an ideal-gas thermometer.

Perhaps the $\langle\, p^2\,\rangle$ question should be posed differently : "Under what conditions will the long-time-averaged kinetic temperatures of all the particles have the same value ?" Any robust disparity in the temperatures (insensitive to small perturbations) makes perpetual motion of the second kind possible. Heat furnished by a "hotter" particle could be used to do work (with an external Carnot Cycle) , returning the unused heat to a "colder" one. Because such a full conversion of heat to work is highly illegal one would necessarily find that attempts to harness the high-temperature heat to do work are doomed unless they would simultaneously cause the temperature difference to disappear. A host of pedagogical problems of this kind seem ideally suited for analysis through the ϕ^4 model and are recommended for further research.

V.   ACKNOWLEDGMENTS

---

[1] K. Aoki and D. Kusnezov, "Bulk Properties of Anharmonic Chains in Strong Thermal Gradients: Nonequilibrium ϕ^4 Theory", Physics Letters A **265**, 250-256 (2000).

[2] K. Aoki and D. Kusnezov, "Nonequilibrium Steady States and Transport In the Classical Lattice ϕ^4 Theory", Physics Letters B **477**, 348-354 (2000).

[3] B. Hu, B. Li, and H. Zhao, "Heat Conduction in One-Dimensional Nonintegrable Systems", Physical Review E **61**, 3828-3831 (2000).

[4] B. L. Holian, W. G. Hoover, and H. A. Posch, "Resolution of Loschmidt's Paradox: The Origin of Irreversible Behavior in Reversible Atomistic Dynamics", Physical Review Letters **59**, 10-13 (1987).

[5] B. Moran, W. G. Hoover, and S. Bestiale, "Diffusion in a Periodic Lorentz Gas", Journal of Statistical Physics **48**, 709-726 (1987).

[6] Wm. G. Hoover, H. A. Posch, K. Aoki, and D. Kusnezov, "Remarks on NonHamiltonian Statistical Mechanics: Lyapunov Exponents and Phase-Space Dimensionality Loss", Europhysics Letters **60**, 337-341 (2002).

[7] W. G. Hoover and H. A. Posch, "Direct Measurement of Lyapunov Exponents", Physics Letters A **113**, 82-84 (1985).

[8] W. G. Hoover and H. A. Posch, "Direct Measurement of Equilibrium and Nonequilibrium Lyapunov Spectra", Physics Letters A **123**, 227-230 (1987).

[9] K. Aoki and D. Kusnezov, "Lyapunov Exponents and the Extensivity of Dimensional Loss for Systems in Thermal Gradients", Physical Review E **68**, 056204 (2003) .

[10] H. A. Posch and W. G. Hoover, "Large-System Phase-Space Dimensionality Loss in Stationary Heat Flows", Physica D **187**, 281-293 (2004).

[11] W. G. Hoover and C. G. Hoover, *Simulation and Control of Chaotic Nonequilibrium Systems*, Section 7.7, pages 204-205 (World Scientific Publishing, Singapore, 2015).

[12] F. Ricci-Tersenghi, "The Solution to the Challenge in 'Time-Reversible Random Number Generators' by Wm. G. Hoover and Carol G. Hoover", arXiv.1305.1805.

[13] W. G. Hoover, B. L. Holian, and H. A. Posch, "Comment I on 'Possible Experiment to Check the Reality of a Nonequilibrium Temperature' ", Physical Review E **48**, 3196-3198 (1993).

[14] Wm. G. Hoover, K. Aoki, C. G. Hoover, and S. V. De Groot, "Time-Reversible Deterministic Thermostats", Physica D **187**, 253-267 (2004).